Biophysical Chemistry 297 (2023) 107007

Contents lists available at ScienceDirect

Biophysical Chemistry

journal homepage: www.elsevier.com/locate/biophyschem

Orexin A, an amphipathic α-helical neuropeptide involved in pleiotropic functions in the nervous and immune systems: Synthetic approach and biophysical studies of the membrane-bound state

Haydn L. Ball [a], Hooda Said [b], Karen Chapman [c], Riqiang Fu [d], Yawei Xiong [e], Joshua A. Burk [f], Daniel Rosenbaum [c], Remi Veneziano [b], Myriam L. Cotten [e,*]

[a] Department of Chemistry, University of Texas Southwestern Medical Center, Dallas, TX 75390, USA
[b] Department of Bioengineering, College of Engineering and Computing, George Mason University, Fairfax, VA 22030, USA
[c] Department of Biophysics, University of Texas Southwestern Medical Center, Dallas, TX 75390, USA
[d] National High Magnetic Field Laboratory, Tallahassee, FL 32310, USA
[e] Department of Applied Science, William & Mary, Williamsburg, VA 23185, USA
[f] Department of Psychological Sciences, William & Mary, Williamsburg, VA 23185, USA

ARTICLE INFO

Keywords:
Anti-inflammatory
Circular dichroism
Hypocretin
Isotopic labeling
Membrane interactions
Neuropeptide
Nuclear magnetic resonance (NMR)
Orexin
Receptor activation
Surface plasmon resonance
Synthesis

ABSTRACT

This research reports on the membrane interactions of orexin A (OXA), an α-helical and amphipathic neuropeptide that contains 33 residues and two disulfide bonds in the N-terminal region. OXA, which activates the orexins 1 and 2 receptors in neural and immune cell membranes, has essential pleiotropic physiological effects, including at the levels of arousal, sleep/wakefulness, energy balance, neuroprotection, lipid signaling, the inflammatory response, and pain. As a result, the orexin system has become a prominent target to treat diseases such as sleep disorders, drug addiction, and inflammation. While the high-resolution structure of OXA has been investigated in water and bound to micelles, there is a lack of information about its conformation bound to phospholipid membranes and its receptors. NMR is a powerful method to investigate peptide structures in a membrane environment. To facilitate the NMR structural studies of OXA exposed to membranes, we present a novel synthetic scheme, leading to the production of isotopically-labeled material at high purity. A receptor activation assay shows that the ^{15}N-labeled peptide is biologically active. Biophysical studies are performed using surface plasmon resonance, circular dichroism, and NMR to investigate the interactions of OXA with phospholipid bilayers. The results demonstrate a strong interaction between the peptide and phospholipids, an increase in α-helical content upon membrane binding, and an in-plane orientation of the C-terminal region critical to function. This new knowledge about structure-activity relationships in OXA could inspire the design of novel therapeutics that leverage the anti-inflammatory and neuro-protective functions of OXA, and therefore could help address neuroinflammation, a major issue associated with neurological disorders such as Alzheimer's disease.

Abbreviations: Acm, acetamidomethyl; AHs, amphipathic helices; cAMP, cyclic adenosine monophosphate; CHAPS, 3-((3-cholamidopropyl) dimethylammonio)-1-propanesulfonate; CD, circular dichroism; CNS, central nervous system; cpm, counts per minute; DIEA, N,N-diisopropylethylamine; DMF, *N,N*-dimethylformamide; DMEM, Dulbecco's modified Eagle medium; EC_{50}, effective concentration to obtain half of the maximal response; GPCR, G-protein coupled receptor; HA, hemagglutinin; HATU, 2-(1H-7-azabenzotriazol-1-yl)-1,1,3,3-tetramethyluronium hexafluorophosphate; HBS, N-2-hydroxyethylpiperazine-N-2-ethane sulfonic acid buffered saline; HBSS, Hanks' balanced salt solution; HEK cells, human embryonic kidney cells; HCl, hydrochloric acid; LHA, lateral hypothalamus area; mRNA, messenger ribonucleic acid; NaOH, sodium hydroxide; NMR, nuclear magnetic resonance; NPY, neuropeptide Y; OXA, orexin A; OXB, orexin B; OX1/2R, orexin 1/2 receptors; RP-HPLC, reverse-phase high-performance liquid chromatography; SPPS, solid phase peptide synthesis; SPR, surface plasmon resonance; SUVs, small unilamellar vesicles; TFA, trifluoroacetic acid; Trt, trityl; YSi, yttrium silicate..

* Corresponding author at: Department of Applied Science, William & Mary, 540 Landrum Drive, #0287, Williamsburg, VA 23185, USA.
E-mail address: mcotten@wm.edu (M.L. Cotten).

https://doi.org/10.1016/j.bpc.2023.107007
Received 6 February 2023; Received in revised form 11 March 2023; Accepted 12 March 2023
Available online 15 March 2023

1. Introduction

In recent years, bioactive peptides that perform a broad range of vital functions at biological membranes have garnered interest in the development of novel therapeutics [1–5]. While these essential biomolecules are highly diversified in terms of sequence and secondary structure, many feature amphipathic helices (AHs) as a conserved building block. AHs promote interactions with membranes, setting the stage for processes that enable functions directly at the level of the membrane (e.g., antimicrobial activity; curvature sensing; membrane remodeling; membrane fusion) or indirectly through the activation of G-protein coupled receptors (GPCRs) implicated in signal transduction pathways [3,6–18]. The key functions and widespread distribution of membrane-interacting bioactive peptides with α-helical character underscore the importance of membrane binding and secondary structure for eliciting crucial biological functions. In this article, we feature structure-activity relationship studies in orexin A (OXA), an amphipathic α-helical peptidic messenger that acts through GPCRs to produce pleiotropic physiological effects in the nervous and immune systems.

It is well established that the membrane environment plays an important role in signal transduction pathways. Clearly, membrane receptors experience interactions that are modulated by the surrounding lipids, with specific lipid domains and species influencing their structures and functions [19–29]. Another important aspect is that the membrane environment constitutes a key platform where ligands first partition before binding to their cognate receptors. Ligand-membrane interactions are believed to be consequential to receptor function for a number of reasons well epitomized in the "membrane compartment theory" proposed by Schwyzer [30–38]. In this view, the target cell membrane induces the bioactive conformation of neuropeptides and the lipids that specifically surround receptors play a selection role by preferentially attracting ligands with complementary physicochemical properties. Hence, the membrane performs the dual catalytic roles of antenna to attract specific ligands in the vicinity of the receptors and chaperone to induce folding into a confirmation conducive to receptor binding and activation. This mechanistic model highlights a fascinating aspect of membrane biophysics where the specific composition of plasma membranes takes on a central role in determining the receptor affinity, and therefore potency of neuropeptides. Due to the lack of information on the membrane- and receptor-bound states of peptidic messengers, it has been challenging to fully explore this paradigm. However, some great strides have been possible thanks to the development of high-resolution methods such as solid-state NMR that are well suited to such demanding structural studies [39–45].

One of the major classes of peptidic messengers studied for its importance in human health includes the orexin family. The two orexin peptides, OXA and orexin B (OXB), were co-discovered by two different research groups [46,47]. Both peptides, also called hypocretins 1 and 2, respectively, originate from the same pro-peptide. OXA and OXB activate two GPCR sub-types belonging to the class A family called orexin receptor 1 (OX1R) and orexin receptor 2 (OX2R) [46,47]. Based on the EC_{50}, OXA is about ten times more active than OXB on OX1R while both peptides are equally potent on OX2R [47]. Intracellular systems that are activated by orexin receptors include enzymes such as phospholipases, diacylglycerol lipase, and adenylyl cyclase, and signaling cascades such as those associated with Ca^{2+}, inositol, and cyclic adenosine monophosphate (cAMP) (for reviews, see references [48, 49]).

Orexin neurons that produce the mRNA of prepro-orexin were initially identified in the lateral hypothalamus area (LHA), which is associated with feeding [46,47]. Later studies demonstrated that orexin neurons project from the LH throughout the central nervous system (CNS), including other areas of the hypothalamus, the cortical and limbic areas, as well as the autonomic and motor systems [50]. Hence, it is not surprising that orexins have been implicated in pleiotropic functions at the levels of sleep-wake regulation, energy homeostasis, cognition, and the processing of emotions, stress, and reward [46–48,51–56]. Notably, the activation of OX1R specifically occurs in the cholinergic and noradrenergic systems in addition to the amygdala and ventromedial nucleus of the hypothalamus [50,56,57]. Given the roles of these brain areas in regulating emotions, pain, feeding, and addiction, OX1R has become a major drug target with potential for treating obesity, anxiety, and drug addiction. This is contrasted by the activation of OX2R that occurs mostly in the paraventricular nucleus and histaminergic neuronal cells of the hypothalamus, and therefore has implications for sleep/wakefulness state and arousal [50,57–60].

More recently, orexins and their receptors were found to be expressed in several peripheral tissues including the adrenals, gastrointestinal tract, pancreas, kidneys, adipose tissues, and reproductive system (for reviews see references [51, 52, 55, 61]). The importance of the orexins for immunity has also been investigated. OXB exhibits antimicrobial effects in combination with the human antimicrobial peptide LL37 [62]. Remarkably, multiple studies document the neuroprotective and immunomodulatory (anti-inflammatory) properties of OXA [48,51,63–66]. In particular, evidence shows the ability of OXA to reduce the neuroinflammatory impact of diets high in saturated fats [48,51,63–66]. The counteracting effects of OXA include reducing lipid peroxidation and apoptosis in hypothalamic cells and regulating the M_1/M_2 phenotype dynamics in microglial cells [64]. As a result, OXA has tremendous therapeutic potential in several immune-related disorders that are associated with or affect the CNS such as narcolepsy, Alzheimer's disease, multiple sclerosis, intestinal/bowel disease, and septic shock [48,65].

With 33 residues, OXA is longer than OXB, which is 28 amino acids long [47]. The two peptides are amidated at the C-terminus and share 46% sequence identity, mainly from having highly conserved C-terminal regions [67–69]. Structure-activity relationship studies have identified that the conserved C-terminus is critical for biological activity [70–73]. While OXB is a linear peptide, OXA contains two intramolecular disulfide bonds between cysteines 6 and 12 and between cysteines 7 and 14, and features an N-terminal pyroglutamic cyclization [47]. The disulfide bonds of OXA have been correlated to its longer half-life compared to OXB [47,74–76]. Interestingly too, the sequence of OXA is more conserved than that of OXB between species [77]. Truncating up to 14 residues from its N-terminus does not fully suppress biological activity while alterations at the C-terminus are strongly inhibitory [70–73].

Both OXA and OXB have been structurally studied by solution NMR in aqueous solution, and in the case of OXA, bound to SDS micelles (Fig. 1) [67–69,78]. While those structures (three for OXA and one for OXB) differ from each other, there is a common feature that the peptides adopt partial α-helical content and have amphipathic character. More specifically, OXB adopts two helices (e.g., helices 1 and 2 in the middle and C-terminal regions, respectively) and OXA features up to three α-helical segments (e.g., helix 1 in the middle region; helices 2 and 3 in the C- and N-terminal regions, respectively), with helix 1 conserved in the three published structures. In 18 mM phosphate buffer at pH 6.0, the peptide is most ordered with three helices, while only two helical segments are observed in 50 mM phosphate buffer at pH 7.0 (helices 1 and 2) and in SDS micelles at pH 5.35 (helices 1 and 3). Another common feature between OXA and OXB is that their structures in buffer display a flexible hinge between helices 1 and 2. In buffer at pH 6.0 and 7.0, both helices 1 and 2 of OXA are amphipathic, and thus could be involved in membrane interactions. It has been noted that the disulfide bonds in the N-terminal region stabilize a hydrophilic turn (RQKT) between helices 3 and 1 [67]. This turn may play a role in OX1R recognition and could explain the stronger affinity of OXA than OXB for this receptor [67]. Out of the three solved conformations of OXA, two are bent and one is straight, while the known structure of OXB is bent. Based on cryo-EM studies complemented with a model from molecular dynamics simulations, OXB bound to OX2R appears to retain some α-helical character [79]. It is expected that either the straight or bent conformation represents the bioactive state that activates the orexin receptors [80,81]. However, there is overall a lack of structural characterization of these

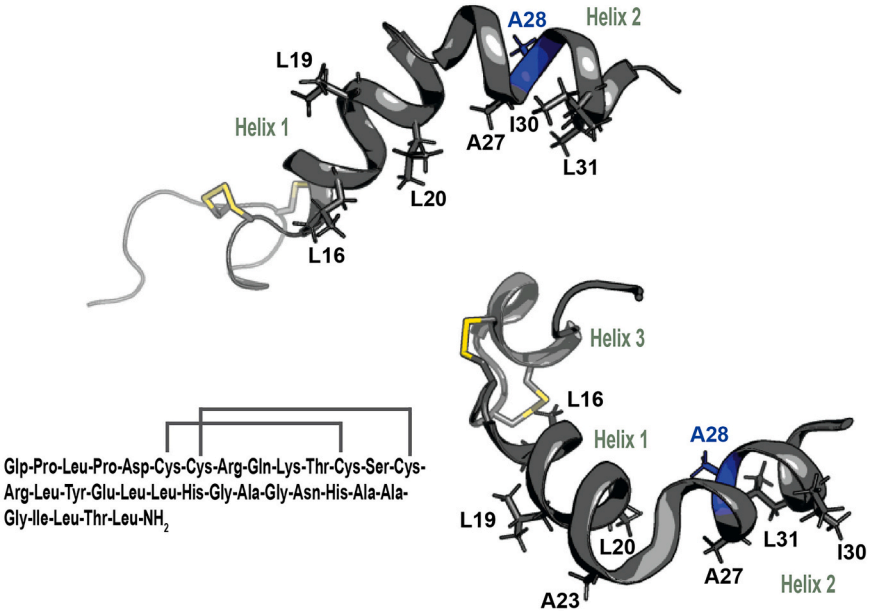

Fig. 1. Amino acid sequences and structural features of OXA previously studied by NMR. Left, bottom. Sequence of OXA. Top, and right, bottom. Structural features of OXA based on structures deposited in the protein data bank. The structure (PDB ID # 1R02) shown on the left corresponds to OXA in 50 mM phosphate buffer at pH 7.0 [58] while the structure shown on the right (PDB ID # 1WSO) is for OXA studied in 18 mM phosphate buffer at pH 6.0 [59]. The helices 1, 2, and 3 are indicated in green while the ^{15}N-labeled Ala28 (A28) is shown in blue. The disulfide bonds appear in yellow. (For interpretation of the references to colour in this figure legend, the reader is referred to the web version of this article.)

peptides in their bioactive conformations and the preceding membrane-bound states.

In this study, we focus on OXA given its enhanced stability compared to OXB, the vital biological functions that it performs, and its ability to be more selective than OXB to OX1R, an intensely investigated drug target. We first present a novel synthetic method to prepare an OXA peptide where the isotopically-labeling is at position 28 in the C-terminal region (highlighted in blue in Fig. 1) and the two disulfide bonds are correctly formed, as demonstrated through a GPCR-activation assay. We then use biophysical methods including circular dichroism (CD), surface plasmon resonance (SPR), and NMR to investigate the interactions of OXA with phospholipid bilayers. Through this approach, the peptide is studied in the presence of zwitterionic (e.g., phosphocholine) and anionic (e.g., phosphoglycerol) phospholipids, which are abundant in the neural cells relevant to its biological function [82,83]. In particular, the use of multilamellar vesicle samples and aligned bilayers in the solid-state NMR study provides orientational information (e.g., tilt and rotational angles of the helix) that is not readily available from isotropic systems, such as micelles [39–42,44]. To our knowledge this is the first investigation of OXA binding to lipid bilayers. The results are discussed in the context of prior studies done on OXA and related neuropeptides to help better understand their bioactive state. The insights gained from these new studies of OXA could inspire the design of novel therapeutics that feature the vital functions performed by OXA.

2. Methods

2.1. Materials

Unless otherwise indicated, chemicals and reagents were purchased from Fisher Scientific (Hampton, NH) and reagent grade (≥ 95% pure). Water was purified using the Millipore MilliQ system (Sigma Aldrich, Saint Louis, MO). Lipids (> 99% pure) were obtained from Avanti Polar Lipids (Alabaster, AL). LIP-1 sensor chip were acquired from Nicoya Lifesciences (Kitchener, Canada). Natural abundance (referred to as "unlabeled") OXA (>95% pure) was purchased from Bachem (Bubendorf, Switzerland).

2.2. Solid phase peptide synthesis and purification of Orexin A

The peptide ^{15}N-A$_{28}$-OXA (pEPLPDCCRQKTCSCRLYELLHGAGN-HAAGILTL-NH$_2$ with C6/C12 and C7/C14 disulfide bonds; MW 3561.2) was manually synthesized using an optimized Fmoc chemistry and a Rink Amide Resin (P3Bio, Louisville, KY). Peptide synthesis grade chemicals were used (≥ 95% pure). Acylations were conducted in 10-mL disposable polypropylene reaction vessels (Biorad, Hercules, CA) using 2-(1H-7-azabenzotriazol-1-yl)-1,1,3,3-tetramethyluronium hexafluorophosphate (HATU) (P3Bio) and N,N-diisopropylethylamine (DIEA) (Sigma-Aldrich), 6-fold excess of amino acid, and Fmoc deprotections with 20% piperidine (Alfa Aesar, Haverhill, MA) in *N*,*N*-dimethylformamide (DMF) (Fisher Scientific). To reduce on-resin secondary structure formation, pseudo-proline dipeptides K10-T11 and L31-T32 (Novabiochem from Sigma-Aldrich) were used at the appropriate points in the synthesis. ^{15}N-labeled Ala protected with an Fmoc group (Cambridge Isotope Laboratories, Tewksbury, MA) was incorporated at residue 28 overnight, using a 2-fold excess. The final coupling featured Boc-protected Pyroglutamic acid (ChemImpex, Wood Dale, IL).

To enable controlled disulfide bridge formation an orthogonal protection approach was adopted. One disulfide pair (Cys7-Cys14) was oxidized by air oxidation after trifluoroacetic acid (TFA) cleavage of the Cys(Trt). The second pair (Cys6-Cys12) was orthogonally protected during this step using the Cys(tBuThio) reagent. The tBuThio protection was selectively removed using tri-n-butyl-phosphine (Alfa Aesar) and then air oxidized [84]. The fully oxidized OXA was purified on a C4 semi-preparative reverse-phase high-performance liquid chromatography (RP-HPLC) column (250 × 10 mm) from Grace (Columbia, MD) on a Waters 600 Preparative HPLC system with buffer A (water/0.045% TFA) and buffer B (acetonitrile/0.036% TFA). The buffers were made with HPLC grade solvents (> 99.9% pure). A gradient from 5 to 100% B was run at a flow rate of 3 mL/min in 120 mins with detection at 220 nm. Analysis of the purified fractions was performed on a Sciex X500B QTOF mass spectrometer and a Shimadzu LC10 HPLC system, using a C18 analytical RP column from Grace (150 × 4.6 mm). The analytical gradient was run from 0% to 100% B in 30 mins, with detection at 220 nm.

Before performing the functional and biophysical studies, the ^{15}N-labeled and unlabeled peptides were dissolved in 0.01 M hydrochloric acid (HCl) to displace the residual TFA counterion carried over from HPLC. After lyophilization and resuspension in water, the peptide

solutions were neutralized with sodium hydroxide (NaOH) and dialyzed to remove excess salt. The lyophilized powders were kept at −20 °C until ready for further analysis. To determine peptide concentration and confirm the amino acid content, amino acid analysis was performed (AAA Service Laboratory, Damascus, OR).

2.3. GPCR activation

The inositol phosphate accumulation assay was used to measure activation of OX2R by the synthesized OXA following a previously published protocol [85]. Human embryonic kidney (HEK) 293 cells were maintained in high-glucose Dulbecco's modified Eagle medium (DMEM) (Sigma-Aldrich) with 5% Fetal Bovine Serum (Corning, Corning, NY) and penicillin-streptomycin (Sigma-Aldrich). Human OX2R was cloned into pcDNA3 with a hemagglutinin (HA) signal followed by a Flag tag at the N-terminus. The receptor and human $G_{\alpha q}$ subunit were co-transfected into HEK293 cells using Lipofectamine 3000 (Thermo Fisher). Twenty four hours after transfection, cells were harvested into growth medium without inositol (MP Biomedicals, Irvine, CA). Myo-[2−^{3}H] inositol (Perkin Elmer, Waltham, MA) was added to about 5 μCi per mL and cells were plated at 30,000 cells per well onto white, 96-well culture plates with clear bottoms (Corning) that had been coated with poly-D-lysine (Sigma-Aldrich). Cells were labeled overnight at 37 °C. To stimulate inositol phosphate production, media was replaced with agonists that had been Hanks' balanced salt solution (HBSS) diluted into (Sigma-Aldrich) containing 10 mM lithium chloride and returned to the incubator for 45 min. Then the plates were placed on ice, agonists were removed and replaced with 10 mM formic acid to lyse the cells. After 30 min, 1.25 mg of polylysine yttrium silicate (YSi) beads (Perkin Elmer) were added to each well. Plates were shaken on an orbital shaker for 30 min at room temperature before reading on a MicroBeta Scintillation Counter (Perkin Elmer).

2.4. POPC liposomes preparation for surface plasmon resonance

Liposomes were prepared according to the thin film hydration method. The lipid 1-palmitoyl-2-oleoyl-sn-glycero-3-phosphocholine (POPC) was prepared at a lipid concentration of 2 mg/mL in chloroform in a flat bottom glass vial then slowly dried under vacuum in a desiccator overnight to obtain a thin and homogeneous lipid film. The film was hydrated in 20 mM HEPES buffered saline (HBS, Sigma Aldrich, St. Louis, MO) containing 150 mM NaCl (pH 7.4) at room temperature for 2 h and gently vortexed prior to the extrusion. Multilamellar vesicle suspensions were extruded using a mini extruder (Avanti Polar Lipids) with two 1 mL gas-tight syringe (Avanti Polar Lipids) through a series of polycarbonate hydrophilic membranes having pore sizes of 200 nm (10 times) and 50 nm (20 times) (Whatman, Buckinghamshire, UK). The hydrodynamic diameter of the small unilamellar vesicles (SUVs) was measured using dynamic light scattering with a ZetaSizer Nano ZS instrument (Malvern Instruments Ltd., Worcestershire, UK). The liposomes were stored at 4 °C prior further use.

2.5. Surface plasmon resonance experiments

The POPC liposome binding kinetic of the OXA peptide was measured with the OpenSPR instrument (Nicoya, Kitchener, ON, Canada). Prior to liposomes loading, the LIP-1 sensor chips were cleaned with three injections of 100 μL of 20 mM 3-((3-cholamidopropyl) dimethylammonio)-1-propanesulfonate (CHAPS) solution (150 μL/min). Liposomes at a concentration of 0.5 mg/mL in N-2-hydroxyethylpiperazine-N-2-ethane sulfonic acid buffered saline (HBS) buffer were injected at a flow rate 20 μL/min for 5 min and left to equilibrate for 5 min. Various concentrations of the OXA peptide diluted in the HBS buffer were then injected at a flow rate of 10 μL/min. The liposomes were removed from the surface using three washes with 20 mM CHAPS detergent (Sigma Aldrich) after each peptide injection and reloaded with liposomes prior to the next peptide injection. The binding kinetic measurements for each concentration of peptide were performed at least in triplicate. The TraceDrawer software was used to fit the kinetic data using a 1:1 Langmuir binding model.

2.6. Circular dichroism experiments

The secondary structure of OXA was monitored in phosphate buffer (3 mM, pH 7.4 and 5.5) by circular dichroism (CD) spectroscopy. The lipid system consisted of POPC and 1-palmitoyl-2-oleoyl-sn-glycero-3-phosphoglycerol (POPG) (Avanti Polar Lipids) mixed in a 3:1 molar ratio. Large unilamellar vesicles (LUVs) were made as previously reported [86]. Briefly, the lipids were co-dissolving in chloroform using a round bottom flask. The solvent was then evaporated under a flow of N_2 gas to form a lipid film that was placed under vacuum overnight. The lipids were then hydrated with the buffer to produce a 5 mM lipid suspension. After 3–4 freeze-thaw cycles, extrusion was performed using an extruder (Avanti Polar Lipids) and 100 nm membranes (Whatman, Florhan Park, NJ). Before mixing with the peptides, the vesicles were diluted down to 2.0–3.0 mM. The P/L ratios were as indicated in the figures, with the peptide being kept at a fixed peptide concentration while the lipid amount was varied. The CD spectra were collected at room temperature on a Jasco J-1500 (Jasco Analytical Instruments, Easton, MD) using parameters that included a 190–260 nm wavelength range, scan speed of 100 nm/min, bandwidth of 1 nm, and accumulation of four scans. For each sample run at a given P/L ratio, a blank containing the buffer and LUVs but no peptide was collected and subtracted from the data obtained in the presence of the peptide. Samples were made in duplicates yielding similar results, with one representative data set being displayed. To calculate the percent α-helical content, the molar ellipticity at 222 nm was used, with an ellipticity of −32,000 deg.·cm^2/dmol for an ideal α-helix [87].

2.7. Preparation of oriented samples for solid-state NMR

Samples containing aligned lipid bilayers and ^{15}N-A_{28} OXA were prepared using a protocol previously developed for membrane-binding peptides [86,88,89]. Briefly, after mixing the 1-palmitoyl-2-oleoyl-sn-glycero-3-phosphatidylethanolamine (POPE)/POPG lipids in chloroform, the solvent was removed under a flow of N_2 gas and vacuum was applied overnight. The lipids POPC/POPG were also used to reconstitute the peptide in membranes, giving rise to similar chemical shift results in the NMR experiments. The lipid film was then hydrated with 1 mL of potassium phosphate buffer (3 mM, pH 7.4) containing OXA (~3 mg). The sample was made at P/L = 1:40 based on the CD studies and maximum α-helical content obtained under this condition. About 2.2 mg of ^{15}N-A_{28} OXA was present in the sample. The mixture was incubated overnight at 40 °C before being spread on glass plates (dimensions 5.7x12x0.03 mm^3 from Matsunami Trading Co., Japan) using a micropipette. The sample was placed in a humidity chamber (>90% using a saturated potassium sulfate solution) until equilibrium was achieved. The slides were re-hydrated at 50% by weight before stacking and inserting into a glass cell (New Era, Vineland, NJ). To maximize the sample volume in the glass cell, about 35–40 glass plates are typically used. A seal was formed using with beeswax (Hampton Research, Aliso Viejo, CA) and incubation was performed at 40 °C until homogeneous hydration was achieved (~5 days).

2.8. ^{15}N solid-state NMR

^{15}N solid-state NMR spectroscopy was performed on a 600 MHz wide bore Bruker instrument with an Avance console at the National High Magnetic Field Laboratory. The data were collected using a low-electrical field probe [90] tuned to ^{1}H and ^{15}N frequencies of 600.12 and 60.81 MHz, respectively. Referencing was done using $(NH_4)_2SO_4$ at 26.8 ppm. The phase-switched cross polarization (CP), which is quite

standard for static experiments and works well for aligned samples, was used [91]. Parameters for CP were as previously used on α-helical peptide-lipid samples, including a 810-μsec contact time and 62.5 kHz decoupling during acquisition [92]. A recycle delay of 4 s and 30,160 transients were employed. During data acquisition, temperature was set to 32 ± 0.1 °C. The error bar is reported as 0.5*FWHM where FWHM is the full width at half maximum.

3. Results

3.1. Synthesis and purification

Solid phase peptide synthesis (SPPS) is widely used to synthesize peptides at high yield and affordable cost. For techniques that require labeling, SPPS is also highly advantageous since it enables the incorporation of labels at selected sites. Here, our goal was to achieve site-specific labeling of OXA in order to use it in NMR structural studies of OXA bound to membranes. However, OXA, a membrane-interacting peptide, presents multiple challenges for SPPS. First, at 33 residues, it is considered a long peptide for SPPS. Second, the peptide contains two disulfide bonds, and thus there is a possibility of scrambled SS bonds if the cysteines are not oxidized in a controlled fashion. Third, it features a hydrophobic sequence. In particular, several motifs could be difficult to couple because secondary structure could form on the resin. This includes the regions containing K10-T11 and L31-T32 dipeptide motifs. For this reason, our strategy included the incorporation of pseudo-pro dipeptides at these specific points to disrupt undesirable secondary structures.

To control the formation of the disulfide bonds present in the native peptide, C_6/C_{12} and C_7/C_{14}, an orthogonal strategy was followed. One pair of Cys was protected with trityl (Trt) and the other pair with tBu-Thio. The first disulfide pair was oxidized in the air after cleavage of Cys (Trt) by TFA. To remove the tBuThio protection, tri-n-butyl-phosphine was used and the second disulfide bond was formed in the air. Following this approach, we were able to produce 13.6 mgs of purified ^{15}N-A_{28} OXA. Another synthesis was also performed, yielding similar results, and therefore showing the reproducibility of the approach. The HPLC chromatogram and mass spectra are shown in **Fig. S1 and** Fig. 2, respectively. The purity is estimated to be >95% based on the combined HPLC and mass spectrometry data.

3.2. Functional assay

OXA activates OX1R and OX2R with similar affinity [47]. To demonstrate that the synthetic ^{15}N-A_{28} OXA could perform function on par with the endogenous ligand, we performed a GPCR-activation assay featuring OX2R. Once activated, the receptor recruits and activates G_q proteins. The efficacy of ^{15}N-A_{28} OXA can thus be determined by monitoring the level of the second messenger inositol phosphate that is produced upon activating $G_{\alpha q}$ protein. As shown in Fig. 3, HEK293 cells overexpressing OX2R are stimulated with ^{15}N-A_{28} OXA, resulting in the expected sigmoidal concentration-response curve. ^{15}N-A_{28} OXA yields an EC_{50} value in the nanomolar range (2.5 ± 0.4 nM) that is comparable to that of the commercial OXA (2.1 ± 0.4 nM). This is in good agreement with the EC_{50} of OXA for OX1R that was previously reported to be 5.0 ± 1.8 nM with this assay [85].

3.3. Evidence for membrane binding

We used SPR to determine the binding kinetics of ^{15}N-A_{28} OXA to POPC liposomes. The POPC liposomes with an average diameter of about 80 nm (**Figs. S1 and S2**) were efficiently loaded on a LIP-1 sensor chip with a consistent level of immobilization across all the experiments and performed with an average of 310 ± 54.5 (mean ± SD) RU (**Fig. S3**). Solutions of OXA at various concentration (from 0.5 μM to 10 μM) in HBS buffer were injected over the liposomes and the equilibrium dissociation constant (K_d) was calculated to be 3.15 μM (Fig. 4). The low K_d in the micromolar range, indicates a strong affinity of the OXA peptide for POPC bilayers.

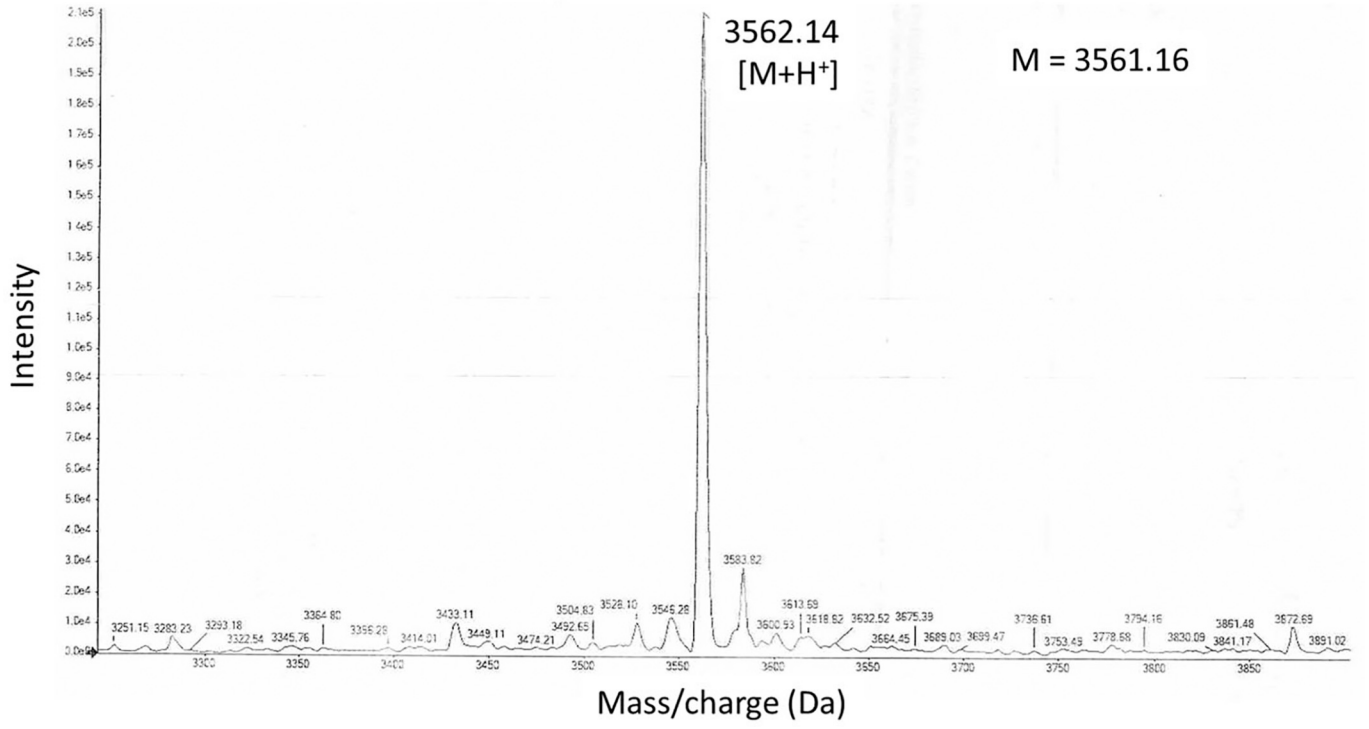

Fig. 2. Mass spectrometry of purified OXA. The data were obtained on a Micromass LR MALDI-TOF instrument. The expected mass/charge is detected for the [M + H^+] adduct of ^{15}N-labeled peptide at 3562.14.

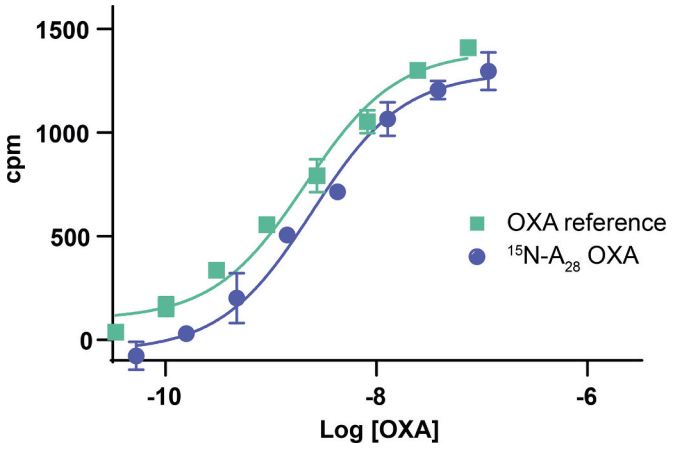

Fig. 3. Functional studies of OXA synthesized with an ^{15}N labeled. The activation of OX2R was determined using an IP_1 accumulation assay. The OXA concentration-response curves were obtained in the presence of increasing concentration of the OXA reference (commercial peptide) and ^{15}N-A_{28} OXA. The count-per-minute (cpm) measurements are displayed for [^{3}H]-inositol accumulated upon OX2R activation. The EC_{50} values of 2.5 ± 0.4 nM and 2.1 ± 0.4 nM for the labeled and commercial peptides, respectively, were determined by fitting the sigmoidal plots. Curves represent the mean ± SD for experiments performed in duplicates. Independent experiments were performed, leading to similar EC_{50} values for the reference and labeled peptides.

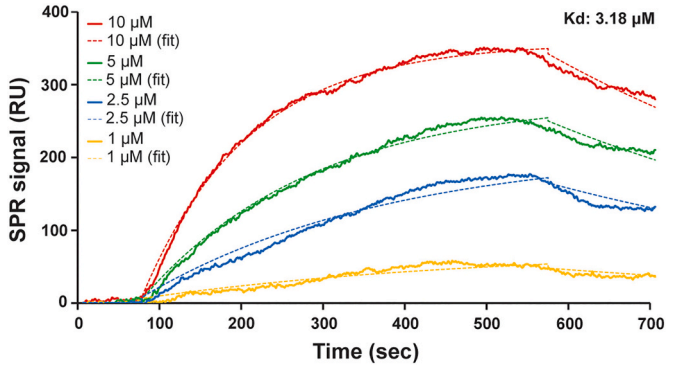

Fig. 4. Representative SPR binding kinetics measurement for OXA interacting with phospholipid surfaces. Four different orexin-A concentrations (1 μM, 2.5 μM, 5 μM, and 10 μM) were injected over immobilized POPC bilayers. The K_d between OXA and POPC bilayers was determined to be 3.18 μM by fitting the binding curves using a 1:1 Langmuir binding model.

3.4. Evidence for α-helical content of OXA bound to phospholipid membranes

Once it was determined that OXA interacts with phospholipids, we carried out CD experiments to monitor the secondary structure of the peptide as a function of peptide-to-lipid (P/L) ratio. Based on previous studies of OXA in buffer and micelles, the peptide adopts partial α-helical content [67–69]. To characterize the α-helical content of OXA bound to lipid membranes, the molar ellipticity obtained by CD at 222 nm was monitored while the P/L ratio was varied from 1:0 to 1:120. Since anionic lipids have previously been used in the biophysical studies of peptides interacting with models of neural membranes [82,83,93–95], we incorporated POPG in the phospholipids used for the CD studies. The data collected at 1:120 used the highest amount of lipids (2.4 mM). At this high concentration of vesicles, scattering can take place, as suggested by the increased amount of noise at wavelengths below 200 nm [96]. As shown in Fig. 5, the α-helical content increases when the P/L varies from 0 to 40 and then stabilizes. At the beginning of the titration, the amount of lipid is low, and thus all of the available membrane surface is covered by OXA molecules while other peptide molecules remain unbound, leading to a low α-helical content. As the titration progresses, the α-helical content increases, reflecting the increased availability of lipids. Under the conditions tested, the maximum α-helical content reached by OXA is about 30%. Kim et al. also reported increased α-helical content upon raising the molar ratio between DPC micelles and peptide from 250 to 625 [67]. Since SPR shows that OXA interacts strongly with phospholipid bilayers, we conclude that the rising α-helical content observed when OXA is added to increasing amounts of phospholipids indicates that the peptide gains α-helical content upon membrane binding. When the end of the titration is reached, sufficient surface area of the bilayer has been made available to the peptide and the α-helical content does not change anymore.

3.5. Evidence for a surface-bound conformation in the presence of phospholipid membranes

Next, we performed NMR experiments on ^{15}N-A_{28} OXA. The label is positioned in helix 2 based on the prior structural studies [67,68]. First, we used solid-state NMR to detect the ^{15}N label in the purified peptide. As shown in **Fig. S5**, a broad powder pattern is observed in agreement with the labeling of A_{28}. Second, we incorporated the labeled peptide in aligned lipid bilayers made of 3:1 POPE/POPG. The sample was placed in the probe so that the bilayer normal was oriented parallel to the static magnetic field, B_0. As indicated in Fig. 6-**B**, a strong resonance is observed at 66.5 ppm. Similar results were obtained with 3:1 POPC/POPG. This is consistent with helix 2 (Fig. 1) in the C-terminal region essential for function lying in an orientation parallel to the membrane surface [97,98]. We note that the ^{15}N NMR signal is broad, suggesting that as detected by NMR, the membrane-bound peptide does not adopt a single, well-defined orientation. Instead, the peptide seems to experience a broad range of orientations [99].

4. Discussion

In this study, we develop a new strategy to achieve the synthesis of ^{15}N-labeled OXA at a high level of purity and investigate the interactions of OXA with phospholipid bilayers. We reveal that OXA gains α-helical content in the presence of bilayers. For the first time, the phospholipid bilayer orientation of OXA is characterized and consistent with the presence of a C-terminal α-helix that lies parallel to the membrane surface. While the structure of OXA bound to its cognate GPCRs remains unknown, this structural study in the presence of bilayers fills some gaps about the conformation that it adopts in the step preceding receptor binding and activation. Since the membrane conformation is believed to be related to that of the bioactive state, the findings highlighted here suggest that the C-terminal region of OXA that is critical for biological function is ordered in preparation for receptor binding.

In an earlier study [100], Söll et al. featured a one-step procedure to synthesize OXA. Their approach relied on the use of iodine to cleave a pair of cysteine protecting groups and to oxidize the cysteines into disulfide bonds. More specifically, the authors used different sidechain protecting groups on the cysteines, so that they could be deprotected and oxidized in a step-wise fashion. C6 and C12 were protected with Acm while C7 and C14 used a Trt protective group. S-Trt was removed during TFA cleavage from the resin. Formation of the first disulfide bond occurred using iodine in acetic acid, which also enabled the removal of the Acm albeit at a slower pace than the oxidation reaction. Thus, the second disulfide bond formed only after the first one was already established. The authors indicated a 35% yield from this procedure.

Following the scheme of Söll et al. [100], we attempted to prepare ^{15}N-labeled OXA but were not as successful in producing significant amount of full length OXA. Furthermore, the oxidation reaction with iodine proved to be challenging to perform given the need to extract the excess iodine with tetrachloromethane, which is highly toxic. To

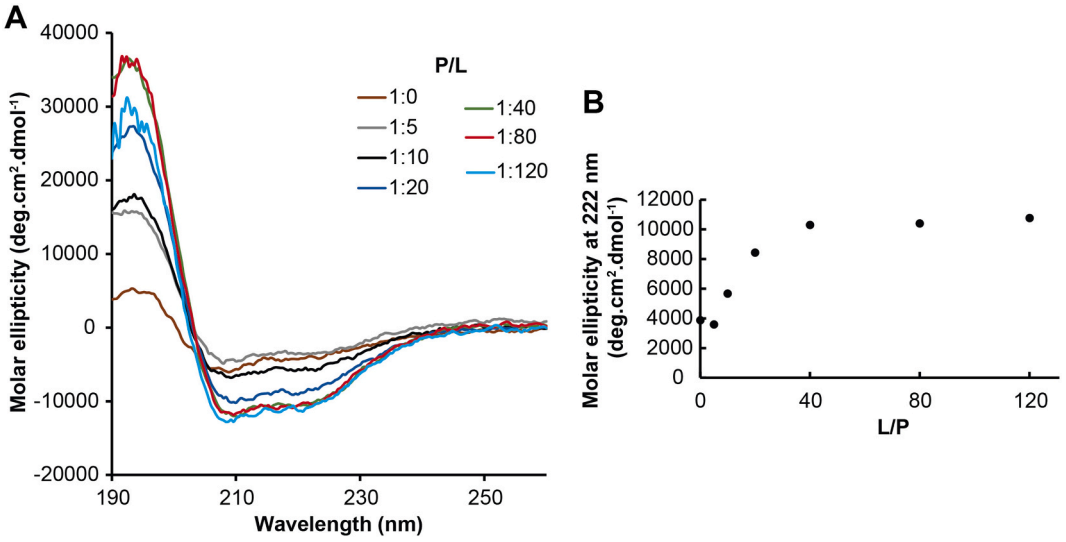

Fig. 5. Structural studies of OXA interacting with phospholipid bilayers. A. CD-monitored titrations of OXA exposed to 3:1 POPC/POPG LUVs. The titrations were done at a fixed concentration of peptide (20 μM) and increasing amounts of LUVs, as indicated. Similar results were obtained at pH 5.5 and 7.4, with the pH 5.5 data shown here. B. The absolute value of the molar ellipticity of OXA as it binds to PC/PG LUVs is shown as a function of the lipid-to-peptide ratio (L/P). Based on this plot, the maximum α-helical content reached by OXA is about 30%.

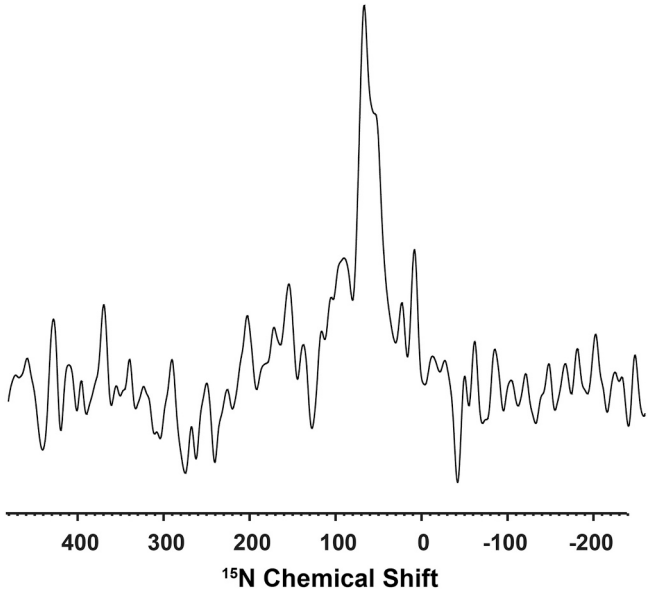

Fig. 6. Bilayer orientation of OXA interacting with phospholipid bilayers. Solid-state NMR spectrum of ^{15}N-A_{28} OXA interacting with hydrated and aligned 3:1 POPE/POPG bilayers. The sample, which was prepared at P/L = 1:40, was placed in the NMR probe with the bilayer normal parallel to the static magnetic field. Since the sample is constituted of aligned lipid molecules, this placement of the sample results in the long axis of the lipid molecules to be oriented parallel to the static magnetic field. Since OXA binds to the lipid bilayers and these are aligned, it gives rise to an anisotropic chemical shift that reflects its orientation with respect to the bilayer normal [97,98]. The chemical shift centered at 66.5 ± 12.5 ppm is consistent with an orientation of the helix containing A_{28} (helix 2) lying parallel to the membrane surface. The data were processed with a Gaussian window function (LB = − 100 Hz, GB = 0.05).

improve the ability to produce full length OXA, we focused on the 15 amino acids of the peptide knowing that building the rest of the peptide on the resin was not a major issue. We identified K10-T11 as a sequence that could be difficult to couple, and thus could benefit from the use of a pseudo-pro dipeptide. This approach, which greatly improved the yield, was also implemented at the level of L31-T32, another place susceptible to difficult coupling. Overall, the use of these two pseudo dipeptides helped enhance the overall yield and crude peptide purity. We also opted for cysteine protecting groups that could be removed under different reaction conditions. As featured by Söll [100], we used the Trt group that can be readily removed during TFA cleavage. To avoid the use of iodine and tetrachloromethane, we selected tBuThio as the protecting group for the other pair of cysteines and used tri-n-butylphosphine to deprotect it. The disulfide bonds were sequentially formed by air oxidation. The resulting product was readily purified by HPLC. While the yield of this approach (about 15%) was lower than that presented by Söll et al. [100], it provided a product with high purity, that was isotopically labeled, and avoided the use of iodine and tetrachloromethane.

To the best of our knowledge, OXA had not previously been studied in the presence of phospholipid bilayers. Three high-resolution structures are available for the solution form of the peptide [67–69]. While they do not entirely agree, they feature a middle helix (helix 1). The structure obtained in 18 mM phosphate buffer at pH 6.0 is the most ordered with three α-helical segments. It shares an N-terminal α-helix with the structure solved in SDS micelles at pH 5.35 and a C-terminal α-helix with the structure characterized in 50 mM phosphate buffer at pH 7.0. This variability in structural content reflects the flexibility of the peptide and possibly a high responsiveness to changing sample conditions (e.g., pH; micelles versus plain buffer; peptide concentration). In all three cases for the solution studies of OXA, the peptide concentrations were relatively high, ranging from 0.76 to 2 mM. However, no oligomeric states were detected, suggesting that high concentration did not induce aggregation as part of these experiments.

Interestingly, the CD spectra displayed in Kim et al. [67] for OXA studied at 80 μM in buffer and in the presence of DPC micelles exhibit a high α-helical content. However, we note that Kim et al. were careful to not interpret their results in terms of percent helical content. Such interpretation could be challenging. Indeed, the molar ellipticity at 222 nm goes below −40,000 deg.cm^2.dmol^{-1} in the presence of 50 and 100 mM DPC. This is stronger than the molar ellipticity observed at 222 nm for proteins that are 100% α-helical (typically in the range of −32,000 to - 39,000 deg.cm^2.dmol^{-1}) [101]. One explanation for the pronounced molar ellipticity of OXA in DPC micelles could be that the sequence of the peptide or its structural arrangement at 80 μM predisposes it to having maximal molar ellipticity that falls outside of the typical range. Alternatively, it could be that the peptide concentration was

underestimated given how difficult it is to accurately determine the concentration of amphipathic peptides. If weight is used, concentrations tend to be overestimated because the peptides carry counterions. If absorbance is used, there could also be some issues if the calculation of concentration uses a standard extinction coefficient since its value can vary as a function of pH and buffer conditions. In our case, we opted for amino acid analysis to characterize peptide concentration, since this was also an excellent way to confirm the amino acid content of the peptide. In our hands, both the commercial and labeled OXA, which successfully underwent amino acid analysis and biological testing, were not α-helical when used at 20 μM and pH 7.4 in 3 mM phosphate buffer. However, addition of phospholipids readily induced the appearance of α-helical content, up to about 30% based on a concentration determined by amino acid analysis. It is unclear if the discrepancy compared to the data obtained by Kim et al. comes from different sample conditions (e.g., buffer concentration; peptide concentration) or methodology for concentration determination. Most importantly, this point of discussion underscores the pitfalls associated with using CD to estimate absolute α-helical content. Fortunately, NMR determines peptide structures at high resolution without involving peptide concentration in the calculations. Accordingly, it is much more reliable to consider the NMR structures to interpret the conformational behaviors of OXA under changing conditions.

Considering the three known solution NMR structures of OXA [67–69], the solid-state NMR data we obtained for OXA in the membrane-bound state agree with the structures solved in buffer at pH 6.0 and 7.0 since they both feature a C-terminal helix. This is interesting since this region is essential for biological activity. This suggests that folding of this region is important for receptor recognition. Other neuropeptides with AHs have been investigated on a structural level. This includes neuropeptide Y (NPY), which activates the Y receptors (for comprehensive reviews, see references [34, 102, 103]). Orexins and NPY share several features besides being essential peptidic messengers with pleiotropic functions, including at the level of feeding. NPY has strong affinity for membranes [104], as shown here for OXA. Furthermore, NPY also exhibits amphipathic α-helical character and a C-terminal region essential for receptor activation [104–106]. While the C-terminal region of NPY is α-helical in solution, its conformation was found to be extended (possibly into a β-sheet) by NMR and docked studies of NPY bound to the Y_1 receptor. In contrast, the central part of the peptide, which was in contact with two extracellular loops, remained α-helical [107]. Hence, conformational rearrangement of a C-terminal α-helix can occur upon insertion in the receptor binding pocket. Future structural studies of OXA in the membrane- and receptor-bound state will be needed to determine if it follows a pattern similar to that of NPY.

5. Conclusion

Given its crucial biological functions and prominent place in drug discovery research, OXA is an important neuropeptide to investigate on a structural level. Here, we synthesized ^{15}N-A_{28} OXA and demonstrated that OXA interacts strongly with phospholipid bilayers. Results from NMR studies with ^{15}N-labeled OXA are consistent with α-helical content in the C-terminal region. These results open the door to future NMR structural studies of the peptide, as needed to characterize its structure bound to membranes and cognate receptors. In particular, it would be interesting to probe the overall peptide structure by placing ^{15}N labels in the N-terminal region. The influence of pH and membrane charge and curvature on the peptide could also be explored by systematically varying the sample conditions and using different sizes of vesicles (e.g., SUVs; LUVs). Using ^{31}P NMR, the impact of the peptide on the membrane organization could be examined to complement the structural studies on the peptide. Deeper knowledge of the bioactive conformation of OXA would be helpful to designing analogs that can be used to leverage its beneficial properties in the CNS, including its immunomodulatory effects, given the pressing need to identify novel therapeutics to treat neurological disorders. This will require additional knowledge regarding the respective roles of the OX1R and OX2R receptors in diseases that implicate OXA. Clearly, OXA is certain to remain an exciting and significant topic of research in the biological sciences.

Author contributions

M.L.C. planned the overall project, including the conceptualization, design of the investigation and methodology, data analysis, project administration, supervision, securing of resources and funding, and writing. H.L.B. designed the synthetic strategy to produce labeled OXA, performed the synthetic work, and obtained the mass spectrometry and HPLC data. The biological assays were designed and performed by K.C. and D.M.R. The SPR experiments were designed and performed by R.V. and H.S. The CD experiments were designed and performed by M.L.C. and Y.X. The solid-state NMR experiments were planned and analyzed by M.L.C. and the samples made by M.L.C. R.F. carried out the solid-state NMR experiments. J.A.B. provided expertise on the biological significance of OXA, which was used by M.L.C. as part of the conceptualization. The manuscript was written by M.L.C. with some method section materials from co-authors. All co-authors provided feedback on the manuscript.

Declaration of Competing Interest

The authors declare no conflict of interest.

Acknowledgments

M.L.C. acknowledges support through William & Mary, including the Mansfield Professorship Award. The solid-state NMR experiments were carried out at the National High Magnetic Field Lab supported by the National Science Foundation Cooperative agreement DMR-2128556 and the State of Florida.

Appendix A. Supplementary data

HPLC of purified OXA; liposomes size as determined by dynamic light scattering; representative data for SPR , and ^{15}N solid-state NMR for ^{15}N-A_{28} orexin A in the powder form. Supplementary data to this article can be found online at [https://doi.org/10.1016/j.bpc.2023.107007].

References

[1] J. Thundimadathil, Cancer treatment using peptides: current therapies and future prospects, J. Amino Acids 2012 (2012), 967347.
[2] T. Uhlig, T. Kyprianou, F.G. Martinelli, C.A. Oppici, D. Heiligers, D. Hills, X. R. Calvo, P. Verhaert, The emergence of peptides in the pharmaceutical business: from exploration to exploitation, EuPA Open Proteom. 4 (2014) 58–69.
[3] A.P. Davenport, C.C.G. Scully, C. de Graaf, A.J.H. Brown, J.J. Maguire, Advances in therapeutic peptides targeting G protein-coupled receptors, Nat. Rev. Drug Discov. 19 (6) (2020) 389–413.
[4] M. Muttenthaler, G.F. King, D.J. Adams, P.F. Alewood, Trends in peptide drug discovery, Nat. Rev. Drug Discov. 20 (2021) 309–325.
[5] K. Fosgerau, T. Hoffmann, Peptide therapeutics: current status and future directions, Drug Discov. Today 20 (1) (2015) 122–128.
[6] H.T. McMahon, J.L. Gallop, Membrane curvature and mechanisms of dynamic cell membrane remodelling, Nature 438 (7068) (2005) 590–596.
[7] B. Antonny, Mechanisms of membrane curvature sensing, Annu. Rev. Biochem. 80 (2011) 101–123.
[8] R.M. Epand, Fusion peptides and the mechanism of viral fusion, Biochim. Biophys. Acta 1614 (1) (2003) 116–121.
[9] E. Strandberg, A.S. Ulrich, AMPs and OMPs: is the folding and bilayer insertion of beta-stranded outer membrane proteins governed by the same biophysical principles as for alpha-helical antimicrobial peptides? Biochim. Biophys. Acta 1848 (9) (2015) 1944–1954.
[10] J. Zimmerberg, M.M. Kozlov, How proteins produce cellular membrane curvature, Nat. Rev. Mol. Cell Biol. 7 (1) (2006) 9–19.
[11] G. Drin, J.F. Casella, R. Gautier, T. Boehmer, T.U. Schwartz, B. Antonny, A general amphipathic alpha-helical motif for sensing membrane curvature, Nat. Struct. Mol. Biol. 14 (2) (2007) 138–146.

[12] M.E. Alzugaray, M.C. Bruno, M.J. Villalobos Sambucaro, J.R. Ronderos, The evolutionary history of the orexin/Allatotropin GPCR family: from Placozoa and Cnidaria to Vertebrata, Sci. Rep. 9 (1) (2019) 10217.
[13] L. McLean, B. Baron, S. Buck, J. Krstenansky, Lipid and membrane interactions of neuropeptide Y, Biochim. Biophys. Acta 1024 (1990) 1–4.
[14] M. Shimizu, Y. Shigeri, Y. Tatsu, S. Yoshikawa, N. Yumoto, Enhancement of antimicrobial activity of neuropeptide Y by N-terminal truncation, Antimicrob. Agents Chemother. 42 (10) (1998) 2745–2746.
[15] J.C. Reubi, Peptide receptors as molecular targets for cancer diagnosis and therapy, Endocr. Rev. 24 (4) (2003) 389–427.
[16] A. Kaiser, I. Coin, Capturing peptide-GPCR interactions and their dynamics, Molecules 25 (20) (2020).
[17] C. Has, S.L. Das, Recent developments in membrane curvature sensing and induction by proteins, Biochim. Biophys. Acta Gen. Subj. 1865 (10) (2021), 129971.
[18] L.E. Jensen, S. Rao, M. Schuschnig, A.K. Cada, S. Martens, G. Hummer, J. H. Hurley, Membrane curvature sensing and stabilization by the autophagic LC3 lipidation machinery, Sci. Adv. 8 (50) (2022) eadd1436.
[19] M. Auger, Biological membrane structure by solid-state NMR, Curr. Iss. Mol. Biol. 2 (2000) 119–124.
[20] G.L. Nicolson, The fluid-mosaic model of membrane structure: still relevant to understanding the structure, function and dynamics of biological membranes after more than 40 years, Biochim. Biophys. Acta 1838 (6) (2014) 1451–1466.
[21] J.M. Ruysschaert, C. Lonez, Role of lipid microdomains in TLR-mediated signalling, Biochim. Biophys. Acta 1848 (9) (2015) 1860–1867.
[22] H. Hong, Role of lipids in folding, Misfolding and function of integral membrane proteins, Adv. Exp. Med. Biol. 855 (2015) 1–31.
[23] K. Simons, J.L. Sampaio, Membrane organization and lipid rafts, Cold Spring Harb. Perspect. Biol. 3 (10) (2011), a004697.
[24] X. Lin, A.A. Gorfe, I. Levental, Protein partitioning into ordered membrane domains: insights from simulations, Biophys. J. 114 (8) (2018) 1936–1944.
[25] I. Marcotte, F. Separovic, A.M.S. Gagne, A multidimensional 1H NMR investigation of the conformation of methionine-enkephalin in fast-tumbling bicelles, Biophys. J. 86 (2004) 1587–1600.
[26] J.C. Bozelli Jr., S.S. Aulakh, R.M. Epand, Membrane shape as determinant of protein properties, Biophys. Chem. 273 (2021), 106587.
[27] J.P. Ulmschneider, J.C. Smith, S.H. White, M.B. Ulmschneider, The importance of the membrane interface as the reference state for membrane protein stability, Biochim. Biophys. Acta Biomembr. 1860 (12) (2018) 2539–2548.
[28] J.H. Lorent, B. Diaz-Rohrer, X. Lin, K. Spring, A.A. Gorfe, K.R. Levental, I. Levental, Structural determinants and functional consequences of protein affinity for membrane rafts, Nat. Commun. 8 (1) (2017) 1219.
[29] A.B. Ouweneel, M.J. Thomas, M.G. Sorci-Thomas, The ins and outs of lipid rafts: functions in intracellular cholesterol homeostasis, microparticles, and cell membranes: thematic review series: biology of lipid rafts, J. Lipid Res. 61 (5) (2020) 676–686.
[30] D.F. Sargent, R. Schwyzer, Membrane lipid phase as catalyst for peptide-receptor interactions, Proc. Natl. Acad. Sci. U. S. A. 83 (1986) 5774–5778.
[31] R. Schwyzer, Molecular mechanism of opioid receptor selection, Biochemistry 25 (1986) 6335–6342.
[32] R. Schwyzer, In search of the 'bio-active conformation'–is it induced by the target cell membrane? J. Mol. Recognit. 8 (1995) 3–8.
[33] R. Schwyzer, P. Moutevelis-Minakakis, S. Kimura, H. Gremlich, Lipid-induced secondary structures and orientations of (Leu5)-enkephalin: helical and crystallographic double-bend conformers revealed by IRATR and molecular modelling, J. Pept. Sci. 3 (1997) 65–81.
[34] R. Bader, O. Zerbe, Are hormones from the neuropeptide Y family recognized by their receptors from the membrane-bound state? Chembiochem. 6 (2005) 1520–1534.
[35] C. O'Connor, K.L. White, N. Doncescu, T. Didenko, B.L. Roth, G. Czaplicki, R. C. Stevens, K. Wüthrich, A. Milon, NMR structure and dynamics of the agonist dynorphin peptide bound to the human kappa opioid receptor, Proc. Natl. Acad. Sci. 112 (38) (2015) 11852–11857.
[36] O.S. Park, J.K. Bang, C. Cheong, Y.H. Jeon, Structure of AQEE-30 of VGF neuropeptide in membrane-mimicking environments, Int. J. Mol. Sci. 23 (22) (2022).
[37] G. Vauquelin, A. Packeu, Ligands, their receptors and ... Plasma membranes, Mol. Cell. Endocrinol. 311 (1–2) (2009) 1–10.
[38] C.T. Szlenk, J.B. Gc, S. Natesan, Does the lipid bilayer orchestrate access and binding of ligands to transmembrane Orthosteric/allosteric sites of G protein-coupled receptors? Mol. Pharmacol. 96 (5) (2019) 527–541.
[39] R. Ketchem, B. Roux, T. Cross, High-resolution polypeptide structure in a lamellar phase lipid environment from solid state NMR derived orientational constraints, Structure 5 (1997) 1655–1669.
[40] Y. Miao, T.A. Cross, Solid state NMR and protein-protein interactions in membranes, Curr. Opin. Struct. Biol. 23 (6) (2013) 919–928.
[41] B. Bechinger, E.S. Salnikov, The membrane interactions of antimicrobial peptides revealed by solid-state NMR spectroscopy, Chem. Phys. Lipids 165 (3) (2012) 282–301.
[42] J. Radoicic, G.J. Lu, S.J. Opella, NMR structures of membrane proteins in phospholipid bilayers, Q. Rev. Biophys. 47 (3) (2014) 249–283.
[43] Y.C. Su, S.H. Li, M. Hong, Cationic membrane peptides: atomic-level insight of structure-activity relationships from solid-state NMR, Amino Acids 44 (3) (2013) 821–833.
[44] B.S. Perrin Jr., Y. Tian, R. Fu, C.V. Grant, E.Y. Chekmenev, W.E. Wieczorek, A. E. Dao, R.M. Hayden, C.M. Burzynski, R.M. Venable, M. Sharma, S.J. Opella, R. W. Pastor, M.L. Cotten, High-resolution structures and orientations of antimicrobial peptides piscidin 1 and piscidin 3 in fluid bilayers reveal tilting, kinking, and bilayer immersion, J. Am. Chem. Soc. 136 (9) (2014) 3491–3504.
[45] F. Separovic, M.-A. Sani (Eds.), Solid-State NMR: Applications in Biomembrane Structure, IOP Publishing, 2020.
[46] L. de Lecea, T.S. Kilduff, C. Peyron, X. Gao, P.E. Foye, P.E. Danielson, C. Fukuhara, E.L. Battenberg, V.T. Gautvik, F.S. Bartlett 2nd, W.N. Frankel, A. N. van den Pol, F.E. Bloom, K.M. Gautvik, J.G. Sutcliffe, The hypocretins: hypothalamus-specific peptides with neuroexcitatory activity, Proc. Natl. Acad. Sci. U. S. A. 95 (1) (1998) 322–327.
[47] T. Sakurai, A. Amemiya, M. Ishii, I. Matsuzaki, R.M. Chemelli, H. Tanaka, S. C. Williams, J.A. Richardson, G.P. Kozlowski, S. Wilson, J.R. Arch, R. E. Buckingham, A.C. Haynes, S.A. Carr, R.S. Annan, D.E. McNulty, W.S. Liu, J. A. Terrett, N.A. Elshourbagy, D.J. Bergsma, M. Yanagisawa, Orexins and orexin receptors: a family of hypothalamic neuropeptides and G protein-coupled receptors that regulate feeding behavior, Cell 92 (4) (1998) 573–585.
[48] A. Couvineau, T. Voisin, P. Nicole, V. Gratio, C. Abad, Y.V. Tan, Orexins as novel therapeutic targets in inflammatory and neurodegenerative diseases, Front. Endocrinol. (Lausanne) 10 (2019) 709.
[49] S.Y. Khoo, R.M. Brown, Orexin/hypocretin based pharmacotherapies for the treatment of addiction: DORA or SORA? CNS Drugs 28 (8) (2014) 713–730.
[50] J.N. Marcus, C.J. Aschkenasi, C.E. Lee, R.M. Chemelli, C.B. Saper, M. Yanagisawa, J.K. Elmquist, Differential expression of orexin receptors 1 and 2 in the rat brain, J. Comp. Neurol. 435 (1) (2001) 6–25.
[51] A. Couvineau, T. Voisin, P. Nicole, V. Gratio, A. Blais, Orexins: a promising target to digestive cancers, inflammation, obesity and metabolism dysfunctions, World J. Gastroenterol. 27 (44) (2021) 7582–7596.
[52] S. Soya, T. Sakurai, Evolution of orexin neuropeptide system: structure and function, Front. Neurosci. 14 (2020) 691.
[53] J. Li, Z. Hu, L. de Lecea, The hypocretins/orexins: integrators of multiple physiological functions, Br. J. Pharmacol. 171 (2) (2014) 332–350.
[54] C.S. Leonard, J.P. Kukkonen, Orexin/hypocretin receptor signalling: a functional perspective, Br. J. Pharmacol. 171 (2) (2014) 294–313.
[55] J.P. Kukkonen, Lipid signaling cascades of orexin/hypocretin receptors, Biochimie 96 (2014) 158–165.
[56] B.M. Razavi, H. Hosseinzadeh, A review of the role of orexin system in pain modulation, Biomed. Pharmacother. 90 (2017) 187–193.
[57] P. Trivedi, H. Yu, D.J. MacNeil, L.H. Van der Ploeg, X.M. Guan, Distribution of orexin receptor mRNA in the rat brain, FEBS Lett. 438 (1–2) (1998) 71–75.
[58] T. Sakurai, The neural circuit of orexin (hypocretin): maintaining sleep and wakefulness, Nat. Rev. Neurosci. 8 (3) (2007) 171–181.
[59] L. Lin, J. Faraco, R. Li, H. Kadotani, W. Rogers, X. Lin, X. Qiu, P.J. de Jong, S. Nishino, E. Mignot, The sleep disorder canine narcolepsy is caused by a mutation in the hypocretin (orexin) receptor 2 gene, Cell 98 (3) (1999) 365–376.
[60] T.C. Thannickal, R.Y. Moore, R. Nienhuis, L. Ramanathan, S. Gulyani, M. S. Aldrich, M. Cornford, J.M. Siegel, Reduced number of Hypocretin neurons in human narcolepsy, Neuron 27 (2000) 469–474.
[61] A. Couvineau, S. Dayot, P. Nicole, V. Gratio, V. Rebours, A. Couvelard, T. Voisin, The anti-tumoral properties of orexin/Hypocretin hypothalamic neuropeptides: an unexpected therapeutic role, Front. Endocrinol. (Lausanne) 9 (2018) 573.
[62] K. Ohta, M. Kajiya, T. Zhu, H. Nishi, H. Mawardi, J. Shin, L. Elbadawi, N. Kamata, H. Komatsuzawa, T. Kawai, Additive effects of orexin B and vasoactive intestinal polypeptide on LL-37-mediated antimicrobial activities, J. Neuroimmunol. 233 (1–2) (2011) 37–45.
[63] C.M. Duffy, J.P. Nixon, T.A. Butterick, Orexin a attenuates palmitic acid-induced hypothalamic cell death, Mol. Cell. Neurosci. 75 (2016) 93–100.
[64] C.M. Duffy, C. Yuan, L.E. Wisdorf, C.J. Billington, C.M. Kotz, J.P. Nixon, T. A. Butterick, Role of orexin a signaling in dietary palmitic acid-activated microglial cells, Neurosci. Lett. 606 (2015) 140–144.
[65] J. Davies, J. Chen, R. Pink, D. Carter, N. Saunders, G. Sotiriadis, B. Bai, Y. Pan, D. Howlett, A. Payne, H. Randeva, E. Karteris, Orexin receptors exert a neuroprotective effect in Alzheimer's disease (AD) via heterodimerization with GPR103, Sci. Rep. 5 (1) (2015) 12584.
[66] T.A. Butterick, J.P. Nixon, C.J. Billington, C.M. Kotz, Orexin a decreases lipid peroxidation and apoptosis in a novel hypothalamic cell model, Neurosci. Lett. 524 (1) (2012) 30–34.
[67] H.Y. Kim, E. Hong, J.I. Kim, W. Lee, Solution structure of human orexin-a: regulator of appetite and wakefulness, J. Biochem. Mol. Biol. 37 (5) (2004) 565–573.
[68] T. Takai, T. Takaya, M. Nakano, H. Akutsu, A. Nakagawa, S. Aimoto, K. Nagai, T. Ikegami, Orexin-a is composed of a highly conserved C-terminal and a specific, hydrophilic N-terminal region, revealing the structural basis of specific recognition by the orexin-1 receptor, J. Pept. Sci. 12 (7) (2006) 443–454.
[69] M. Miskolzie, G. Kotovych, The NMR-derived conformation of orexin-a: an orphan G-protein coupled receptor agonist involved in appetite regulation and sleep, J. Biomol. Struct. Dyn. 21 (2) (2003) 201–210.
[70] J.G. Darker, R.A. Porter, D.S. Eggleston, D. Smart, S.J. Brough, C. Sabido-David, J. C. Jerman, Structure–activity analysis of truncated orexin-a analogues at the orexin-1 receptor, Bioorg. Med. Chem. Lett. 11 (5) (2001) 737–740.
[71] S. Ammoun, T. Holmqvist, R. Shariatmadari, H.B. Oonk, M. Detheux, M. Parmentier, K.E.O. Åkerman, J.P. Kukkonen, Distinct recognition of OX₁ and OX₂receptors by orexin peptides, J. Pharmacol. Exp. Ther. 305 (2) (2003) 507–514.
[72] M. Lang, R.M. Söll, F. Dürrenberger, F.M. Dautzenberg, A.G. Beck-Sickinger, Structure-activity studies of orexin a and orexin B at the human orexin 1 and

orexin 2 receptors led to orexin 2 receptor selective and orexin 1 receptor preferring ligands, J. Med. Chem. 47 (5) (2004) 1153–1160.
[73] N.A. German, A.M. Decker, B.P. Gilmour, B.F. Thomas, Y. Zhang, Truncated Orexin Peptides: Structure–Activity Relationship Studies, ACS Med. Chem. Lett. 4 (12) (2013) 1224–1227.
[74] R.A. España, B.A. Baldo, A.E. Kelley, C.W. Berridge, Wake-promoting and sleep-suppressing actions of hypocretin (orexin): basal forebrain sites of action, Neuroscience 106 (4) (2001) 699–715.
[75] J.P. Kukkonen, Physiology of the orexinergic/hypocretinergic system: a revisit in 2012, Am. J. Phys. Cell Phys. 304 (1) (2013) C2–32.
[76] I.Z. Shahid, A.A. Rahman, P.M. Pilowsky, Orexin and central regulation of cardiorespiratory system, Vitam. Horm. 89 (2012) 159–184.
[77] M. Shibahara, T. Sakurai, T. Nambu, T. Takenouchi, H. Iwaasa, S.I. Egashira, M. Ihara, K. Goto, Structure, tissue distribution, and pharmacological characterization of Xenopus orexins, Peptides 20 (10) (1999) 1169–1176.
[78] J.H. Lee, E. Bang, K.J. Chae, J.Y. Kim, D.W. Lee, W. Lee, Solution structure of a new hypothalamic neuropeptide, human hypocretin-2/orexin-B, Eur. J. Biochem. 266 (3) (1999) 831–839.
[79] C. Hong, N.J. Byrne, B. Zamlynny, S. Tummala, L. Xiao, J.M. Shipman, A. T. Partridge, C. Minnick, M.J. Breslin, M.T. Rudd, S.J. Stachel, V.L. Rada, J. C. Kern, K.A. Armacost, S.A. Hollingsworth, J.A. O'Brien, D.L. Hall, T. P. McDonald, C. Strickland, A. Brooun, S.M. Soisson, K. Hollenstein, Structures of active-state orexin receptor 2 rationalize peptide and small-molecule agonist recognition and receptor activation, Nat. Commun. 12 (1) (2021) 815.
[80] A. Heifetz, O. Barker, G.B. Morris, R.J. Law, M. Slack, P.C. Biggin, Toward an understanding of agonist binding to human Orexin-1 and Orexin-2 receptors with G-protein-coupled receptor modeling and site-directed mutagenesis, Biochemistry 52 (46) (2013) 8246–8260.
[81] L. Karhu, A. Turku, H. Xhaard, Modeling of the OX1R–orexin-A complex suggests two alternative binding modes, BMC Struct. Biol. 15 (1) (2015) 9.
[82] I. Marcotte, M. Ouellet, M. Auger, Insights on the interaction of met-enkephalin with negatively charged membranes–an infrared and solid-state NMR spectroscopic study, Chem. Phys. Lipids 127 (2) (2004) 175–187.
[83] M.F. Sciacca, S.A. Kotler, J.R. Brender, J. Chen, D.K. Lee, A. Ramamoorthy, Two-step mechanism of membrane disruption by Abeta through membrane fragmentation and pore formation, Biophys. J. 103 (4) (2012) 702–710.
[84] N.J.C.M. Beekman, W.M.M. Schaaper, G.I. Tesser, K. Dalsgaard, S. Kamstrup, J.P. M. Langeveld, R.S. Boshuizen, R.H. Meloen, Synthetic peptide vaccines: palmitoylation of peptide antigens by a thioester bond increases immunogenicity, J. Pept. Res. 50 (5) (1997) 357–364.
[85] J. Hellmann, M. Drabek, J. Yin, J. Gunera, T. Pröll, F. Kraus, C.J. Langmead, H. Hübner, D. Weikert, P. Kolb, D.M. Rosenbaum, P. Gmeiner, Structure-based development of a subtype-selective orexin 1 receptor antagonist, Proc. Natl. Acad. Sci. U. S. A. 117 (30) (2020) 18059–18067.
[86] E.Y. Chekmenev, B.S. Vollmar, K.T. Forseth, M.N. Manion, S.M. Jones, T. J. Wagner, R.M. Endicott, B.P. Kyriss, L.M. Homem, M. Pate, J. He, J. Raines, P. L. Gor'kov, W.W. Brey, D.J. Mitchell, A.J. Auman, M. Ellard-Ivey, J. Blazyk, M. Cotten, Investigating molecular recognition and biological function at interfaces using piscidins, antimicrobial peptides from fish, Biochim. Biophys. Acta 1758 (2006) 1359–1372.
[87] S.A. Lee, Y.K. Kim, S.S. Lim, W.L. Zhu, H. Ko, S.Y. Shin, K.S. Hahm, Y. Kim, Solution structure and cell selectivity of piscidin 1 and its analogues, Biochemistry 46 (12) (2007) 3653–3663.
[88] S.D. Paredes, S. Kim, M.T. Rooney, A.I. Greenwood, K. Hristova, M.L. Cotten, Enhancing the membrane activity of Piscidin 1 through peptide metallation and the presence of oxidized lipid species: implications for the unification of host defense mechanisms at lipid membranes, Biochim. Biophys. Acta Biomembr. 1862 (7) (2020), 183236.
[89] E.Y. Chekmenev, S.M. Jones, Y.N. Nikolayeva, B.S. Vollmar, T.J. Wagner, P. L. Gor'kov, W.W. Brey, M.N. Manion, K.C. Daugherty, M. Cotten, High-field NMR studies of molecular recognition and structure-function relationships in antimicrobial piscidins at the water-lipid bilayer interface, J. Am. Chem. Soc. 128 (2006) 5308–5309.
[90] P.L. Gor'kov, E.Y. Chekmenev, C. Li, M. Cotten, J.J. Buffy, N.J. Traaseth, G. Veglia, W.W. Brey, Using low-E resonators to reduce RF heating in biological samples for static solid-state NMR up to 900 MHz, J. Magn. Reson. 185 (2007) 77–93.
[91] S.M. Zhang, B.H. Meier, S. Appelt, M. Mehring, R.R. Ernst, Transient oscillations in phase-switched Cross-polarization experiments, J. Magn. Reson. A 101 (1) (1993) 60–66.
[92] R. Fu, E.D. Gordon, D.J. Hibbard, M. Cotten, High resolution heteronuclear correlation NMR spectroscopy of an antimicrobial peptide in aligned lipid bilayers: peptide−water interactions at the water−bilayer interface, J. Am. Chem. Soc. 131 (31) (2009) 10830–10831.
[93] S. Bera, R.K. Kar, S. Mondal, K. Pahan, A. Bhunia, Structural Elucidation of the Cell-Penetrating Penetratin Peptide in Model Membranes at the Atomic Level: Probing Hydrophobic Interactions in the Blood–Brain Barrier, Biochemistry 55 (35) (2016) 4982–4996.
[94] M.C. Nicastro, D. Spigolon, F. Librizzi, O. Moran, M.G. Ortore, D. Bulone, P.L. S. Biagio, R. Carrotta, Amyloid β-peptide insertion in liposomes containing GM1-cholesterol domains, Biophys. Chem. 208 (2016) 9–16.
[95] S. Bera, N. Gayen, S.A. Mohid, D. Bhattacharyya, J. Krishnamoorthy, D. Sarkar, J. Choi, N. Sahoo, A.K. Mandal, D. Lee, A. Bhunia, Comparison of synthetic neuronal model membrane mimics in amyloid aggregation at atomic resolution, ACS Chem. Neurosci. 11 (13) (2020) 1965–1977.
[96] H. Chakraborty, B.R. Lentz, A simple method for correction of circular dichroism spectra obtained from membrane-containing samples, Biochemistry 51 (5) (2012) 1005–1008.
[97] S.J. Opella, F.M. Marassi, Structure determination of membrane proteins by NMR spectroscopy, Chem. Rev. 104 (2004) 3587–3606.
[98] J. Wang, J. Denny, C. Tian, S. Kim, Y. Mo, F. Kovacs, Z. Song, K. Nishimura, Z. Gan, R. Fu, J.R. Quine, T.A. Cross, Imaging membrane protein helical wheels, J. Magn. Reson. 144 (1) (2000) 162–167.
[99] E. Chekmenev, B. Vollmar, M. Cotten, Can antimicrobial peptides scavenge around a cell in less than a second? Biochim. Biophys. Acta 1798 (2010) 228–234.
[100] R. Söll, A.G. Beck-Sickinger, On the synthesis of orexin A: a novel one-step procedure to obtain peptides with two intramolecular disulphide bonds, J. Pept. Sci. 6 (8) (2000) 387–397.
[101] Y. Wei, A.A. Thyparambil, R.A. Latour, Protein helical structure determination using CD spectroscopy for solutions with strong background absorbance from 190 to 230nm, Biochim. Biophys. Acta 1844 (12) (2014) 2331–2337.
[102] S.L. Parker, A. Balasubramaniam, Neuropeptide Y Y2 receptor in health and disease, Br. J. Pharmacol. 153 (3) (2008) 420–431.
[103] F. Reichmann, P. Holzer, Neuropeptide Y: A stressful review, Neuropeptides 55 (2016) 99–109.
[104] L.R. McLean, S.H. Buck, J.L. Krstenansky, Examination of the role of the amphipathic alpha-helix in the interaction of neuropeptide Y and active cyclic analogues with cell membrane receptors and dimyristoylphosphatidylcholine, Biochemistry 29 (8) (1990) 2016–2022.
[105] A.G. Beck-Sickinger, H.A. Wieland, H. Wittneben, K.D. Willim, K. Rudolf, G. Jung, Complete L-alanine scan of neuropeptide Y reveals ligands binding to Y1 and Y2 receptors with distinguished conformations, Eur. J. Biochem. 225 (3) (1994) 947–958.
[106] S.A. Monks, G. Karagianis, G.J. Howlett, R.S. Norton, Solution structure of human neuropeptide Y, J. Biomol. NMR 8 (4) (1996) 379–390.
[107] Z. Yang, S. Han, M. Keller, A. Kaiser, B.J. Bender, M. Bosse, K. Burkert, L. M. Kögler, D. Wifling, G. Bernhardt, N. Plank, T. Littmann, P. Schmidt, C. Yi, B. Li, S. Ye, R. Zhang, B. Xu, D. Larhammar, R.C. Stevens, D. Huster, J. Meiler, Q. Zhao, A.G. Beck-Sickinger, A. Buschauer, B. Wu, Structural basis of ligand binding modes at the neuropeptide Y Y(1) receptor, Nature 556 (7702) (2018) 520–524.